Impact of Ga Addition to InSn Solder on ReBCO Joint Performance

Nooshin Goodarzi, Kévin Berger, Alexander Molodyk, Mark Ainslie, Tayebeh Mousavi

Impact of Ga Addition to InSn Solder on ReBCO Joint Performance

Nooshin Goodarzi, Kévin Berger, Alexander Molodyk, Mark Ainslie, *Senior Member, IEEE*, and Tayebeh Mousavi, *Member, IEEE*

***Abstract*—Reliable, robust, low-resistance joints are essential for long-length ReBCO conductors used in high-field superconducting magnets. Yet, common solder joints, such as those made with InSn, suffer from limited mechanical robustness and degradation. This study investigates the influence of adding gallium (Ga) as a minor alloying element (1-7 wt.%) to the eutectic InSn solder for joining commercial ReBCO (YBCO) coated-conductor tapes. Face-to-face lap joints were fabricated using In-Sn-Ga solders and characterized in terms of electrical resistance, microstructure, and mechanical properties. Adding Ga to the eutectic InSn solder decreased the melting points, which is beneficial for joining delicate YBCO tapes. The results showed the formation of a Ga-rich interfacial layer with a $CuGa_2$ composition, leading to a slight increase in the joint electrical resistance compared to binary eutectic InSn. However, mechanical testing revealed that moderate Ga contents (in the range of 1-3 wt.%) improved the joint strength by up to 46% compared to binary eutectic InSn solder. These results indicate that controlled Ga additions can mechanically reinforce the joint without severe electrical degradation, providing a practical approach towards stronger, more reliable joints for ReBCO magnet applications.**

***Index Terms*—Joints, ReBCO conductors, superconducting magnets, microstructure, interfacial layer, mechanical testing, electrical degradation.**

I. INTRODUCTION

REBCO tapes carry large currents under strong magnetic fields, making them ideal for high-field magnets [1]. However, their limited manufacturing length (<200m) requires numerous low-resistance joints for persistent magnet operation [2], [3]. Among joining methods, soldering is the most practical for ReBCO tapes because of its simplicity, reliability, low resistivity, and adaptability to large-scale applications [4]-[7]. The soldering parameters, including the type of solder, require to be precisely designed to create a continuous low-resistance path between the YBCO tapes without degrading these sensitive and brittle tapes at high temperatures [4], [8]-[10]. Hence, a proper solder material with a low melting point, low resistivity and suitable mechanical properties is crucial for the reliable operation of soldered joints [11]-[13]. These properties are controlled by the solder composition and its microstructure upon solidification [14], [15]. The type of solder has been widely studied in the literature for YBCO tapes, including eutectic PbSn [4], [16], [17], InSn [4], [17]-[19], SAC305 [5], [11], and InAg [5]. Among these solders, Pb-free alloys are environmentally friendly and much more desirable for magnet technologies [4], [5], [20]. Sn-based alloys are among the favorite Pb-free solders in joining technology; particularly, the eutectic InSn alloy ($In_{52}Sn_{48}$) has greatly attracted due to its low melting temperature (118 °C), low electrical resistivity, high ductility, good wettability, and long fatigue life, with rather well-known thermal properties compared to other similar options, making it a desirable candidate for joining ReBCO tapes [4], [21]-[23]. However, interfacial reactions at the solder/Cu interface and in the solder matrix end in the formation of brittle, hard intermetallic compounds (IMCs), causing failure of the solder joints [23].

In practical applications, superconducting magnets are generally faced with large electromagnetic forces and thermal stresses, so their components, including the joints, need to have sufficient mechanical strength to provide a reasonably long service life [20], [24]-[27]. Therefore, optimizing both the solder composition and the joining parameters can ensure the formation of joints with high reproducibility, low resistance, and sufficient mechanical strength for superconductive applications. One possible approach to further improve the properties of binary InSn solder is the addition of a third element to form a ternary alloy [18]. It has been shown for solders that adding an element to a binary solder can reduce the melting point, which is profitable for YBCO joints [28], [29]. Gallium (Ga) is a potential additive, which has an inherent low melting point (29.8 °C), is non-toxic, and possesses excellent wetting ability, allowing it to wet most materials without the use of flux [30]-[32]. Tsui et al. [4] also suggested In-Sn-Ga ternary alloys, such as Galinstan, as promising candidates for fabricating demountable joints, since these alloys can form connections at room temperature and be easily detached upon remelting. This study investigates the effect of small Ga additions to binary eutectic InSn solder on the microstructural, electrical, and mechanical properties of YBCO solder joints.

II. EXPERIMENT

The YBCO tape used in this work is a commercial 4 mm-width tape (FFJ-4807-R), manufactured by Faraday Factory Japan (FFJ). Fig. 1 shows the backscattered electron (BSE) image of this tape, along with a line-scan analysis across all layers and a schematic representation of the tape's structure. As observed, the tape has a multilayer structure containing a

Manuscript received October 13, 2025. (*Corresponding author: Nooshin Goodarzi)* Nooshin Goodarzi, Mark Ainslie, and Tayebeh Mousavi are with the Department of Engineering, King's College London, London WC2R 2LS, U.K. (e-mail: nooshin.goodarzi@kcl.ac.uk, mark.ainslie@kcl.ac.uk, and tayebeh.mousavi@kcl.ac.uk). Kevin Berger is with Université de Lorraine, GREEN, F-54000 Nancy, France (e-mail: kevin.berger@univ-lorraine.fr). Alexander Molodyk is with Faraday Factory Japan LLC, Tokyo, Japan (a.molodyk@faradaygroup.com).

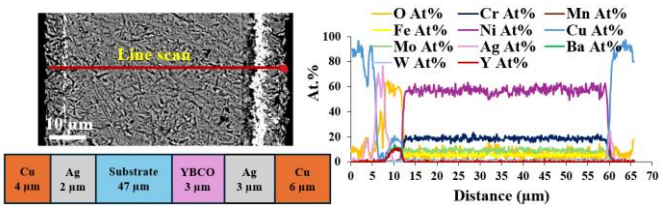

Fig. 1. BSE micrograph of FFJ-4807-R tape cross-section, along with line-scan analysis of the tape and its schematic structure.

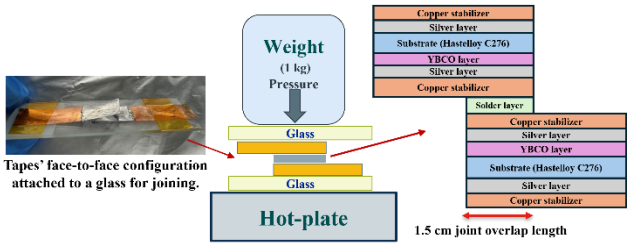

Fig. 2. Schematic illustration of the joint on the hot plate under applied pressure, showing the joint configuration and multilayer structure.

Hastelloy substrate, YBCO layer, two Ag overlayers, and two Cu stabilizers.

The eutectic composition of InSn alloy ($In_{52}Sn_{48}$) was prepared and employed as a Pb-free, binary solder for joining the YBCO tapes. To evaluate the effect of adding Ga to the solder to form a ternary alloy, four different ternary solder compositions, listed in Table I, were prepared in alumina crucibles heated on a temperature-controlled hot plate. The melting temperature of the fabricated solders during solidification was analyzed through differential scanning calorimetry (DSC) at a heating/cooling rate of 10 °C/min under a nitrogen atmosphere.

TABLE I
SOLDER MATERIALS USED IN THIS STUDY

Solder	Chemical composition
InSn	In52Sn48
InSnGa1	In51.48Sn47.52Ga1
InSnGa3	In50.44Sn46.56Ga3
InSnGa5	In49.4Sn45.6Ga5
InSnGa7	In48.36Sn44.64Ga7

A. Tape preparation and joining procedure

The YBCO tapes were cut and thoroughly cleaned with ethanol and acetone to remove surface contaminants. A thin layer of rosin soldering flux was immediately applied to the tape surfaces to prevent surface oxidation, improve wettability, and ensure the formation of a thin, homogeneous solder layer in the joint region. Following surface preparation, the tapes were briefly dipped into a molten solder bath and assembled in an overlapped face-to-face configuration on a glass substrate through Kapton tape, creating a joint area with 1.5 cm in length. The joint was then placed on a hot plate at a temperature determined by DSC analysis under a light pressure of one kg load, and subsequently cooled at a rate of about 12 °C/min (Fig. 2).

B. Joint characterization

The cross-sections of the joints were characterized through a Zeiss scanning electron microscope (SEM) operating at 20 kV accelerating voltage, combined with an Oxford Instruments energy-dispersive X-ray spectroscopy (EDS) and Aztec software. The joint resistance (R_j) was evaluated using the standard four-probe method in liquid nitrogen and under self-field conditions, using a DC power supply. To connect the voltage taps to the sample, two conductive stainless steel flat clips were used to avoid thermal stress generation and stripping between the tape, which are common issues when soldering the voltage taps [7], [33], [34]. The mechanical strength of the 1.5-cm joint was evaluated using uniaxial tensile tests conducted at room temperature. For each solder composition, four joint samples were fabricated and tested under identical testing conditions, using an Instron universal testing machine with a 500 N load cell, pneumatic grips, and serrated jaws, at a crosshead speed of 1 mm/min. Engineering strain of the specimen was determined from the machine's crosshead displacement divided by the initial gauge length. Engineering stress was also calculated by dividing the applied force by the cross-sectional area of a single tape (width × thickness).

III. RESULTS AND DISCUSSIONS

The DSC results shown in Fig. 3 demonstrate that the addition of Ga to eutectic InSn solder effectively reduces the solder's melting temperature, which is advantageous for joining thermally sensitive YBCO tapes. The melting temperatures of the InSn, InSnGa1, InSnGa3, InSnGa5, and InSnGa7 solders were obtained 119.87 °C, 113.10 °C, 99.68 °C, 89.55 °C, and 83.89 °C, respectively. In addition to lowering the melting temperature, Ga addition broadens the melting range, consistent with observations reported in the literature [35]. This progressive reduction in melting temperature with increasing Ga content can be primarily attributed to Ga's intrinsically low melting point. The broadened melting range at higher Ga contents indicates increased compositional heterogeneity and non-equilibrium solidification, which may promote phase segregation and affect interfacial reactions. Hence, while reduced soldering temperatures are beneficial for minimizing thermal degradation of YBCO tapes, excessive Ga additions may lead to Ga segregation and non-uniform microstructures as the alloy composition deviates further from the eutectic InSn system, which solidifies more uniformly upon cooling.

A. Joint microstructure

The quality and performance of soldered lap joints between YBCO tapes are significantly influenced by the joint's microstructure, particularly within the solder region as well as at the solder/tape interface. The BSE/SEM image of the InSn solder joint in Fig. 4(a) shows the formation of a uniform and dense solder layer between the tapes with a continuous connection at the interface between the solder and the copper stabilizer. No porosity or cracks can be seen at the interface between the solder and tapes on both sides, indicating that the joint process, especially the initial tape preparation, provides a

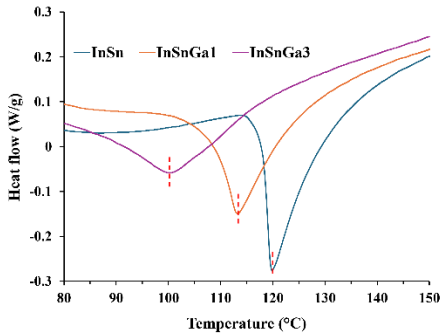

Fig. 3. DSC curves of selected fabricated solders used in this study.

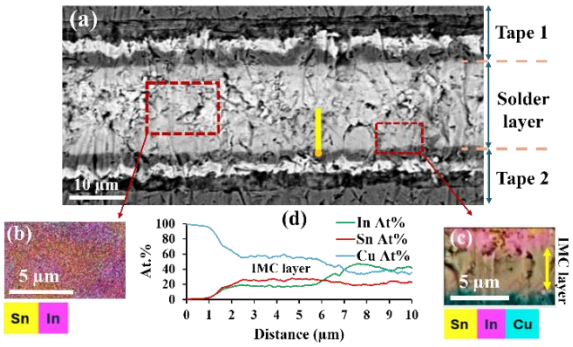

Fig. 4. (a) BSE/SEM micrograph of the InSn solder joint, along with EDS analyses including (b and c) elemental mapping, and (d) line-scan analysis.

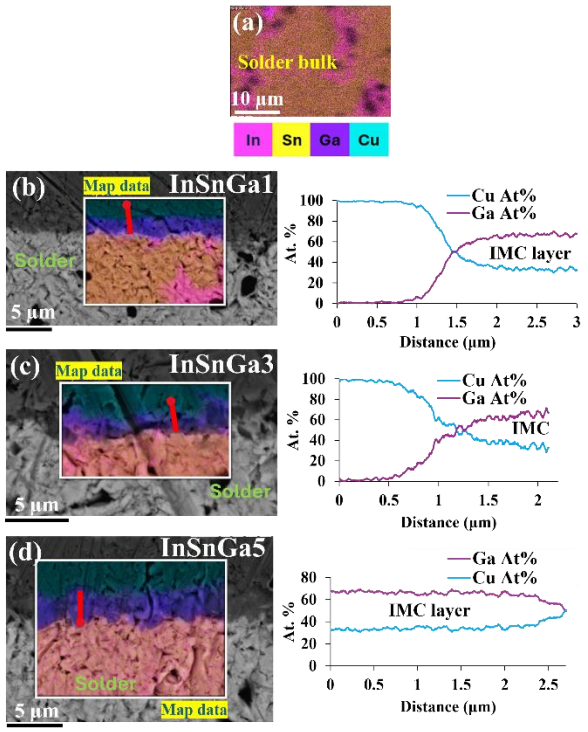

Fig. 5. (a) BSE/SEM micrograph of ternary solder area for InSnGa1 joint, along with EDS analyses (elemental mapping and line scan) of the solder/tape interface for (b) InSnGa1, (c) InSnGa3, (d) InSnGa5 joints.

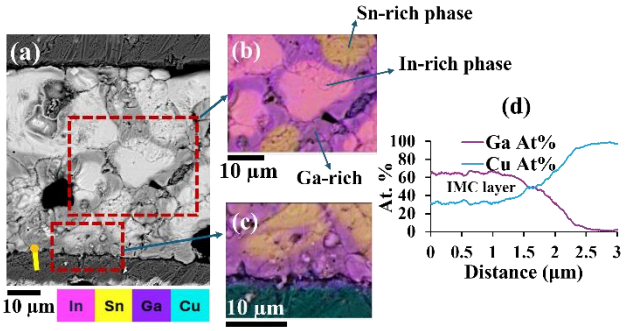

Fig. 6. (a) BSE/SEM micrograph of ternary solder region for InSnGa7 joint, (b) elemental mapping of the solder, (c) elemental mapping of the interface, and (d) line scan analysis of the solder/tape interface.

strong wettability between the tape and InSn solder. Fig. 4(a) also shows a uniform solder thickness of 15 µm across the joint area, with no damage to the tapes as a result of optimized temperature and pressure during the soldering process. The EDS results (mapping data) for the solder bulk in Fig. 4(b) reveal the formation of a two-phase structure, including In-rich (β) and Sn-rich (γ) phases in the bulk of solder, as a result of the eutectic InSn solidification [36]. Fig. 4(c) map data and Fig. 4(d) line-scan data at the interface suggest a few-micron-thick IMC interfacial layer between the solder and Cu stabilizer of the tape. It is reported that during soldering below 200 °C, a main IMC species, $Cu_2(In,Sn)$, is formed at the eutectic In-Sn solder/Cu interface [22]. In the current study, the EDS data, including point and line-scan analyses, confirm this result as well.

The elemental mapping of the solder bulk for the InSnGa1 joint shown in Fig. 5(a) indicates that no Ga is present inside the solder bulk. The EDS analyses in Fig. 5(b-d) suggest that Ga segregates from the solder and reacts with the Cu stabilizer to likely form a thin, continuous $CuGa_2$ IMC layer at the solder/Cu interface, consistent with previous reports [30], [37]. Owing to Ga's strong affinity for Cu, it preferentially diffuses to the interface, thereby altering the interfacial structure and properties compared with those of the binary InSn solder joint. The SEM/EDS results for InSnGa7 solder joint in Fig. 6 indicate that increasing the Ga content leads to additional Ga diffusion into the solder bulk. During solidification, In-rich and Sn-rich phases form first, while excess Ga remains liquid, embedding the solid phases in a Ga-rich phase that solidifies upon further cooling. This phase segregation leads to microstructural heterogeneity, likely degrading mechanical performance by introducing soft, weak regions of low-melting-point Ga-rich phases within the solder matrix. The line-scan analysis of the interface in Fig. 6(d) also suggests the formation of $CuGa_2$ IMC layer at the Cu/solder interface. Thus, the interfacial IMC layer remains thin and continuous even at higher Ga concentrations of 7 wt.%.

B. Joint electrical resistance

The electrical properties of the tape itself were first evaluated using the standard four-probe transport method with a criterion of 1 µV/cm. The n value and critical current (I_c) along the length of the tape at 77 K under self-field conditions were obtained as 34.18 and 138.78 A, respectively (Fig. 7). The joint exhibits an ohmic behavior in currents below I_c, with voltage increasing linearly with current. Hence, the joint resistance was determined from the slope of the V-I curves below I_c. Fig. 8(a) presents the corresponding

measurement data, obtained from four-probe tests on samples at 77 K under self-field conditions. Based on the slopes of each line, the resistivity values for the joints were determined and presented in Fig. 8(b), showing values in the range of 206-358 nΩ·cm^2. The joints made by eutectic InSn solders in the literature were reported to have a resistivity in the range of 80-700 nΩ·cm^2, depending on the tapes [5]. The resistivity values of our joints are within the lower part of this range. The results indicate that increasing the Ga content in the solder increases the joint resistance. It means that the addition of 1, 3, and 5 wt.% Ga leads to an increase in the joint resistivity by 16.6%, 28.7%, and 73.7%, respectively. The joint resistance is the sum of different resistive components, including all the layers and interfaces shown in Figs. 4-6. This increase in joint resistance is likely due to the formation of a higher-resistance interfacial layer between the solder and copper stabilizer ($R_{solder/Cu}$), resulting from the participation of Ga in the interfacial reaction and formation of $CuGa_2$ interfacial barrier, compared to the interfacial resistance in the binary InSn solder system associated with $Cu_2(In,Sn)$ layer. Although Ga addition leads to an increase in joint resistivity, the magnitude of this increase remains moderate for Ga contents up to 3 wt.% (< 29%). However, at 5 wt.% Ga, the resistivity increase becomes significant (73.7%), indicating that excessive Ga additions are detrimental to the joint's electrical performance. Several studies in the literature presenting joint resistance measured at both 77 K and 4.2 K reported that the joint resistance generally decreases substantially from liquid nitrogen to liquid helium temperatures [38]. Since the joint resistances typically decrease at lower temperatures, the relative impact of Ga-induced resistance increases is expected to be less remarked under actual magnet operating conditions.

C. Joint mechanical properties at room temperature

The mechanical behaviour of the fabricated solder joints was studied using tensile testing to evaluate the impact of Ga addition on their mechanical strength. All joints failed within the joint area. Fig. 9(a) presents the stress-strain curve for all the samples. In this test, the applied axial load along the tape length is transferred as shear stress across the overlap joint area. According to the results for the joint tension at failure shown in Fig. 9(b), adding Ga to eutectic InSn solder improves the mechanical properties of the joints compared with the InSn solder joint. The results also indicate that adding up to 3 wt.% Ga to the binary InSn solder enhances the joint mechanical strength by 46%, while further Ga addition decreases the joint strength. Thus, an optimum Ga content of about 1-3 wt.% in the eutectic InSn solder improves the solder joint mechanical properties. The improvement in joint strength for Ga additions up to 3 wt.% can be related to the formation of a thin, continuous $CuGa_2$ IMC layer that enhances interfacial bonding and promotes more effective stress transfer across the joint. However, further Ga addition leads to the formation of low-melting-point Ga-rich phases within the solder bulk. These phases are mechanically softer and weaker, increasing microstructural heterogeneity and reducing the overall load-bearing capacity of the joint. Under tensile loading, strain localization is therefore more likely to occur within these Ga-rich regions, promoting joint failure.

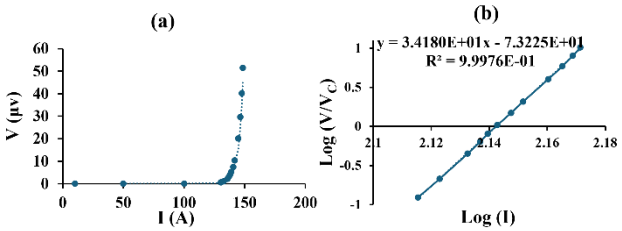

Fig. 7. (a) V-I curve of the FFJ tape, (b) n value and I_c calculations.

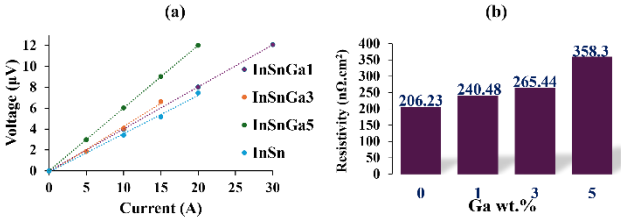

Fig. 8. (a) V-I curves of the joints obtained through the four-probe measurement at 77 K and under self-field conditions; (b) bar-chart of resistivity values for the fabricated joints.

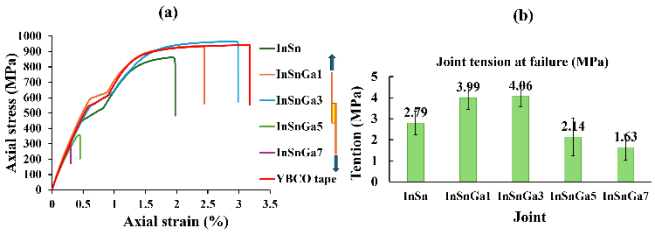

Fig. 9. (a) Engineering stress-strain curves of all samples; (b) mean joint tension at failure for each solder composition, (error bars represent the standard deviation of four joints prepared and tested under the same conditions).

IV. Conclusion

The impact of Ga addition to the InSn solder on the microstructure, electrical and mechanical properties of FFJ YBCO joints was investigated. Based on the DSC results, adding Ga to the eutectic InSn solder decreased the melting point, which is profitable for joining susceptible YBCO tapes. All joints exhibited a uniform and thin solder layer between the tapes, with no obvious damage to the tape's structure. The addition of Ga to InSn solder led to the formation of a thin Ga-rich interface layer composed of $CuGa_2$ between the solder and the Cu layer of the tapes. Consequently, the overall resistance slightly increased with increasing Ga content. However, the addition of 1-3 wt.% Ga enhanced the joint mechanical strength, with 3 wt.% Ga resulting in a 46% increase in tensile strength. Excessive Ga content (above 3 wt.%) reduced the strength, indicating an optimum range for reinforcement. These results suggest that In-Sn-Ga (Ga ≤ 3 wt.%) solders provide reduced soldering temperatures, maintain acceptable low-temperature electrical performance, and improve mechanical strength, thereby benefiting magnet applications and extending their service life.

REFERENCES

[1] S. Mukoyama, A. Nakai, H. Sakamoto, S. Matsumoto, G. Nishijima, M. Hamada, *et al*., "Superconducting joint of REBCO wires for MRI magnet," *J. Phys.: Conf. Ser.*, vol. 1054, Jul. 2018, Art. no. 012038.

[2] H. Maeda, J.-I. Shimoyama, Y. Yanagisawa, Y. Ishii, and M. Tomita, "The MIRAI program and the new super-high field NMR initiative and its relevance to the development of superconducting joints in Japan," *IEEE Trans. Appl. Supercond.*, vol. 29, no. 5, Aug. 2019.

[3] G. D. Brittles, T. Mousavi, C. R. M. Grovenor, C. Aksoy, and S. C. Speller, "Persistent current joints between technological superconductors," *Supercond. Sci. Technol.*, vol. 28, no. 9, 2015, Art. no. 093001.

[4] Y. Tsui, E. Surrey, and D. Hampshire, "Soldered joints—An essential component of demountable high temperature superconducting fusion magnets," *Supercond. Sci. Technol.*, vol. 29, no. 7, Jul. 2016, Art. no. 075005.

[5] M. Skarba, M. Pekarčíková, L. Frolek, E. Cuninková, and M. Necpal, "Thermal cycling of (Re)BCO-based superconducting tapes joined by lead-free solders," *Materials*, vol. 14, no. 4, 2021, Art. no. 872.

[6] A. Preuss, W. H. Fietz, F. Immel, S. Kauffmann-Weiss, and M. J. Wolf, "Critical current degradation of coated conductors under soldering conditions," *IEEE Trans. Appl. Supercond.*, vol. 28, no. 4, Jun. 2018.

[7] D. Huang, H. Gu, Z. Dong, H. Shang, W. Xu, T. Li, *et al*., "Study on electromechanical properties of solder jointed YBCO coated conductors with etched copper stabilizer under axial tension," *IEEE Trans. Appl. Supercond.*, vol. 30, no. 1, Jan. 2020.

[8] Y. Tsui, R. Mahmoud, E. Surrey, and D. Hampshire, "Superconducting and mechanical properties of low-temperature solders for joints," *IEEE Trans. Appl. Supercond.*, vol. 26, no. 3, Apr. 2016.

[9] N. A. A. M. Amin, D. A. Shnawah, S. M. Said, M. F. M. Sabri, and H. Arof, "Effect of Ag content and the minor alloying element Fe on the electrical resistivity of Sn–Ag–Cu solder alloy," *J. Alloys Compd.*, vol. 599, pp. 114–120, 2014.

[10] Y. Zhang, R. C. Duckworth, T. T. Ha, and M. J. Gouge, "Solderability study of RABiTS-based YBCO coated conductors," *Physica C*, vol. 471, nos. 15–16, pp. 772–776, 2011.

[11] M. Drienovský, E. Michalcová, M. Pekarčíková, M. Palcut, L. Frolek, P. Gogola, *et al*., "Induction soldering of coated conductor high-temperature superconducting tapes with lead-free solder alloys," *IEEE Trans. Appl. Supercond.*, vol. 28, no. 4, Jun. 2018.

[12] Y. Chen, L. Fu, W. Wang, J. Xu, F. Ni, G. Lin, *et al*., "A generalized model of HTS–HTS joint resistance for superconducting magnets," *IEEE Trans. Appl. Supercond.*, vol. 34, no. 8, Nov. 2024, pp. 1–4.

[13] M. Zhao, L. Zhang, Z. Q. Liu, M. Y. Xiong, and L. Sun, "Structure and properties of Sn–Cu lead-free solders in electronics packaging," *Sci. Technol. Adv. Mater.*, vol. 20, no. 1, pp. 421–444, 2019.

[14] H. R. Kotadia, P. D. Howes, and S. H. Mannan, "A review: On the development of low melting temperature Pb-free solders," *Microelectron. Reliab.*, vol. 54, nos. 6–7, pp. 1253–1273, 2014.

[15] M. Mueller, S. Wiese, M. Roellig, and K. J. Wolter, "Effect of composition and cooling rate on the microstructure of SnAgCu-solder joints," in *Proc. Electron. Compon. Technol. Conf.*, 2007, pp. 1160–1166.

[16] J. Lu, K. Han, W. R. Sheppard, Y. L. Viouchkov, K. W. Pickard, and W. D. Markiewicz, "Lap joint resistance of YBCO coated conductors," *IEEE Trans. Appl. Supercond.*, vol. 21, no. 3, Jun. 2011.

[17] C. A. Baldan, U. R. Oliveira, A. A. Bernardes, V. P. Oliveira, C. Y. Shigue, and E. Ruppert, "Electrical and superconducting properties in lap joints for YBCO tapes," *J. Supercond. Nov. Magn.*, vol. 26, no. 5, pp. 1465–1469, 2013.

[18] N. Goodarzi, K. Berger, A. Molodyk, M. Ainslie, T. Mousavi, "Development of Ag-Added InSn Solders for ReBCO Joints," *IEEE Trans. Appl. Supercond.*, vol. 36, no. 5, Aug. 2026, pp. 1–5.

[19] T. Mousavi, C. Aksoy, C. R. M. Grovenor, and S. C. Speller, "Microstructure and superconducting properties of Sn–In and Sn–In–Bi alloys as Pb-free superconducting solders," *Supercond. Sci. Technol.*, vol. 29, no. 1, Jan. 2016.

[20] S. Zhang, F. Li, G. Yang, S. Xu, Z. Han, Z. Fan, *et al*., "Enhanced electrical and mechanical performances of soldered joint between copper stabilized REBCO superconducting tapes," *IEEE Trans. Appl. Supercond.*, vol. 29, no. 5, Aug. 2019.

[21] D. G. Kim and S. B. Jung, "Interfacial reactions and growth kinetics for intermetallic compound layer between In–48Sn solder and bare Cu substrate," *J. Alloys Compd.*, vol. 386, nos. 1–2, pp. 151–156, 2005.

[22] P. Shang, F. Tian, and Z. Q. Liu, "Identification and evolution of intermetallic compounds formed at the interface between In–48Sn and Cu during liquid soldering reactions," *Metals*, vol. 14, no. 2, 2024, Art. no. 165.

[23] G. Aurelio, S. A. Sommadossi, and G. J. Cuello, "Crystal structure of Cu–Sn–In alloys around the η-phase field studied by neutron diffraction," *J. Electron. Mater.*, vol. 41, no. 11, pp. 3156–3163, 2012.

[24] S. Ito, H. Hashizume, N. Yanagi, and H. Tamura, "Advanced high-temperature superconducting magnet for fusion reactors: Segment fabrication and joint technique," *Fusion Eng. Des.*, vol. 136, pp. 890–895, 2018.

[25] V. N. Gladky, S. S. Kozub, A. T. Veshchikov, and U. Escher, "Thermal contraction of superconducting magnet materials," *Cryogenics*, vol. 35, no. 1, pp. 25–31, 1995.

[26] S. Kwak, M. Park, W. Kim, S. Hahn, S. Lee, J. Lee, *et al*., "The optimal design of 600 kJ SMES magnet based on stress and magnetic field analysis," *IEEE Trans. Appl. Supercond.*, vol. 18, no. 2, Jun. 2008.

[27] L. Liu, Y. Zhu, X. Yang, T. Qiu, and Y. Zhao, "Delamination properties of YBCO tapes under shear stress along the width direction," *IEEE Trans. Appl. Supercond.*, vol. 26, no. 6, Sep. 2016.

[28] T. Mousavi, C. Aksoy, C. R. M. Grovenor, and S. C. Speller, "Phase evolution of superconducting Sn–In–Bi solder alloys," *IEEE Trans. Appl. Supercond.*, vol. 26, no. 3, Apr. 2016.

[29] C. Aksoy, T. Mousavi, G. Brittles, C. R. M. Grovenor, and S. C. Speller, "Lead-free solders for superconducting applications," *IEEE Trans. Appl. Supercond.*, vol. 26, no. 3, Apr. 2016.

[30] S. Liu, K. Sweatman, S. McDonald, and K. Nogita, "Ga-based alloys in microelectronic interconnects: A review," *Materials*, vol. 11, no. 2, 2018, Art. no. 248.

[31] P. D. Sonawane, V. K. B. Raja, K. Palanikumar, E. A. Kumar, N. Aditya, and V. Rohit, "Effects of gallium, phosphorus and nickel addition in lead-free solders: A review," *Mater. Today: Proc.*, vol. 33, pp. 5272–5276, 2020.

[32] Y. Plevachuk, V. Sklyarchuk, S. Eckert, G. Gerbeth, and R. Novakovic, "Thermophysical properties of the liquid Ga–In–Sn eutectic alloy," *J. Chem. Eng. Data*, vol. 59, no. 3, pp. 757–763, 2014.

[33] M. J. Dedicatoria, Z. Bautista, H. S. Shin, and K. D. Sim, "Note: Effective measurement of retained Ic in evaluating electromechanical properties of high temperature superconductor tapes by the voltage tap clipping technique," *Rev. Sci. Instrum.*, vol. 86, no. 9, 2015, Art. no. 096102.

[34] H. S. Shin, A. Nisay, M. Dedicatoria, and K. D. Sim, "Establishment of an easy Ic measurement method of HTS superconducting tapes using clipped voltage taps," *Prog. Supercond. Cryogenics*, vol. 16, no. 2, pp. 13–18, 2014.

[35] I. Černičková, L. Ďuriška, M. Drienovský, Y. Plevachuk, P. Švec, P. Danišovičová, *et al*., "Influence of gallium addition on the microstructure, thermal behavior, mechanical and electrical properties of SAC305 lead-free solder and solder joints," *J. Mater. Res. Technol.*, vol. 39, 2025.

[36] Y. Shu, T. Ando, Q. Yin, G. Zhou, and Z. Gu, "Phase diagram and structural evolution of tin/indium (Sn/In) nanosolder particles: From a non-equilibrium state to an equilibrium state," *Nanoscale*, vol. 9, no. 34, pp. 12601–12611, 2017.

[37] C. J. Wu, P. P. Huang, L. Zhang, X. Y. Guo, M. Chen, N. Jiang, *et al*., "The effect of Ga on interfacial reactions and intermetallic evolution in SnBiGaIn quaternary alloys," *J. Alloys Compd.*, vol. 1037, 2025.

[38] X. Tian, H. Suo, Z. Zhang, M. Ye, L. Wang, J. Liu, *et al*., "Meter-length REBCO ultralow resistance joint for the gigahertz NMR magnet," *Superconductivity*, vol. 12, 2024.